ELSEVIER

Organic Electronics 2 (2001) 143–154

Organic Electronics

www.elsevier.com/locate/orgel

Characterization of bis(1,2,5-thiadiazolo)-*p*-quinobis(1,3-dithiole) thin films grown by organic molecular beam deposition

Jiangeng Xue [a], Jingui Qin [b], Peter V. Bedworth [b], Karen Kustedjo [b], Seth R. Marder [b,c], Stephen R. Forrest [a,*]

[a] *Department of Electrical Engineering, Center for Photonics and Optoelectronic Materials (POEM), Princeton University, Princeton, NJ 08544, USA*

[b] *Beckman Institute, California Institute of Technology, Pasadena, CA 91125, USA*

[c] *Department of Chemistry, University of Arizona, Tucson, AZ 85721, USA*

Received 26 March 2001; received in revised form 9 May 2001; accepted 21 May 2001

Abstract

Crystalline thin films of the organic compound, bis(1,2,5-thiadiazolo)-*p*-quinobis(1,3-dithiole) (BTQBT) were grown by the ultrahigh vacuum process of organic molecular beam deposition on various substrates including highly ordered pyrolytic graphite, Si(0 0 1), glass and thermal silicon dioxide films on Si. In situ reflection high-energy electron diffraction, scanning electron microscopy, atomic force microscopy, X-ray diffraction, temperature-dependent photoluminescence spectroscopy, and electrical conductivity measurements were employed to characterize the various properties of the films. We find that ordered, polycrystalline films of the planar BTQBT molecules can be grown on a variety of substrates. The BTQBT molecules stack on substrates with their stacking axis perpendicular to the substrate plane. The degree and extent of film ordering strongly depends on the growth conditions: higher growth rates favor more ordered and uniform films. The room-temperature electrical conductivity of the films is $(1.2 \pm 0.1) \times 10^{-3}$ and $(7.5 \pm 0.4) \times 10^{-4}$ S cm^{-1} perpendicular and parallel to the substrate surface, respectively. Both the remarkably high value of conductivity and its small anisotropy are explained in terms of the unusual crystal structure of BTQBT.

PACS: 61.10. -i; 61.14.Hg; 61.16.Bg; 72.80.Le

Keywords: Organic molecular beam deposition; bis(1,2,5-thiadiazolo)-*p*-quinobis(1,3-dithiole) (BTQBT); Quasiepitaxy; Organic thin film; X-ray diffraction; Electrical conductivity

1. Introduction

Organic molecular crystals generally have low electrical conductivity due to the weak van der Waals forces which are typically responsible for intermolecular interactions [1]. However, by introducing chalcogen atoms such as sulfur and

* Corresponding author. Tel.: +1-609-258-4532; fax: +1-609-258-7272.

E-mail address: forrest@ee.princeton.edu (S.R. Forrest).

1566-1199/01/$ - see front matter
PII: S1566-1199(01)00020-9

selenium into organic compounds with extended π-electron systems, the intermolecular interactions can be significantly strengthened. This can serve to increase the conductivity by broadening the conduction energy levels in the material, leading to the development of incipient band-like properties such as has been observed in materials such as pentacene, tetracene [2] and 3,4,9,10-perylenetetracarboxylic dianhydride (PTCDA) [3]. While these materials generally are characterized by strong anisotropies in their electrical and optical properties, introducing chalcogen atoms may effectively couple molecules in all directions, thus reducing such spatial variations. For example, bulk samples of the sulfur-containing bis(1,2,5-thiadiazolo)-*p*-quinobis(1,3-dithiole) (BTQBT), shown in Fig. 1(a), have been reported to have an unusually high and nearly isotropic conductivity of 10^{-3} $S\,cm^{-1}$ [4–6] and a Hall mobility of 4 $cm^2\,V^{-1}\,s^{-1}$ at room temperature [7,8]. The crystal structure of BTQBT (Fig. 1(b)) reveals that the sulfur atoms in neighboring molecules are spaced at only 3.26 Å [4], which is significantly shorter than the sum of their van der Waals radii, i.e., 3.70 Å. Such short S···S contacts (see the dotted lines in Fig. 1(b)) form a tight two-dimensional network with strong intermolecular interactions in the solid state. Indeed, an incipient band structure was observed with the width of the highest occupied molecular orbital (HOMO) band equal to 0.4 eV, measured using angle-resolved photoemission spectroscopy [9–11]. In this sense, BTQBT might be a "transitional" material between one-dimensional, or insulator-like organic molecular crystals (with highly localized electrons) and conventional semiconductors (with three dimensionally delocalized electronic states). Hence it is of fundamental interest to investigate the optical and electronic properties of such a material, and to correlate these properties to the material structure in both the bulk and thin film.

This paper reports a detailed study of the structural, optical and electrical properties of BTQBT thin films, grown by the ultrahigh vacuum (UHV) process of organic molecular beam deposition (OMBD). In past work, OMBD has been used to grow organic thin films of many archetype molecular compounds, such as PTCDA [12]. It has been shown that an ordered organic overlayer can be achieved by OMBD growth in spite of significant incommensurality between the substrate and thin film lattices. This so-called "quasiepitaxial growth" is believed to be a general property of a large range of planar molecules which are bonded primarily by van der Waals forces to the substrate [13].

The paper is organized as follows. Section 2 is a description of the thin film growth and various techniques used to characterize the film properties. These include in situ reflection high-energy electron diffraction (RHEED), scanning electron microscopy (SEM), atomic force microscopy (AFM), X-ray diffraction (XRD), temperature-dependent photoluminescence (PL) spectroscopy, and temperature-dependent electrical conductivity. In Section 3, we present results on the evolution of thin film growth, and the structural, optical and electrical properties of OMBD-grown BTQBT films. The thin-film growth mode and its dependence on growth conditions, as well as comparisons of the electrical properties of bulk and thin film BTQBT, are discussed in Section 4. Finally we summarize our results in Section 5.

2. Experimental

2.1. Thin film growth

The BTQBT source material was synthesized by a Wittig–Horner reaction as previously reported [4,14]. Following synthesis, the material was successively purified for two cycles (each cycle lasting several days to a week) by gradient sublimation [12] prior to loading it into the UHV deposition system with a base pressure $<10^{-8}$ Pa. The OMBD effusion cell containing the source material was continuously maintained at an elevated temperature of 180 °C during the period when these experiments were carried out, thus ensuring that the material remained pure and free of moisture. The Knudsen cell was heated to a temperature between 260 and 330 °C, to achieve a deposition rate between 0.1 and 4 Å/s. The deposition rate was monitored using a calibrated quartz crystal positioned close to the sample holder. The chamber

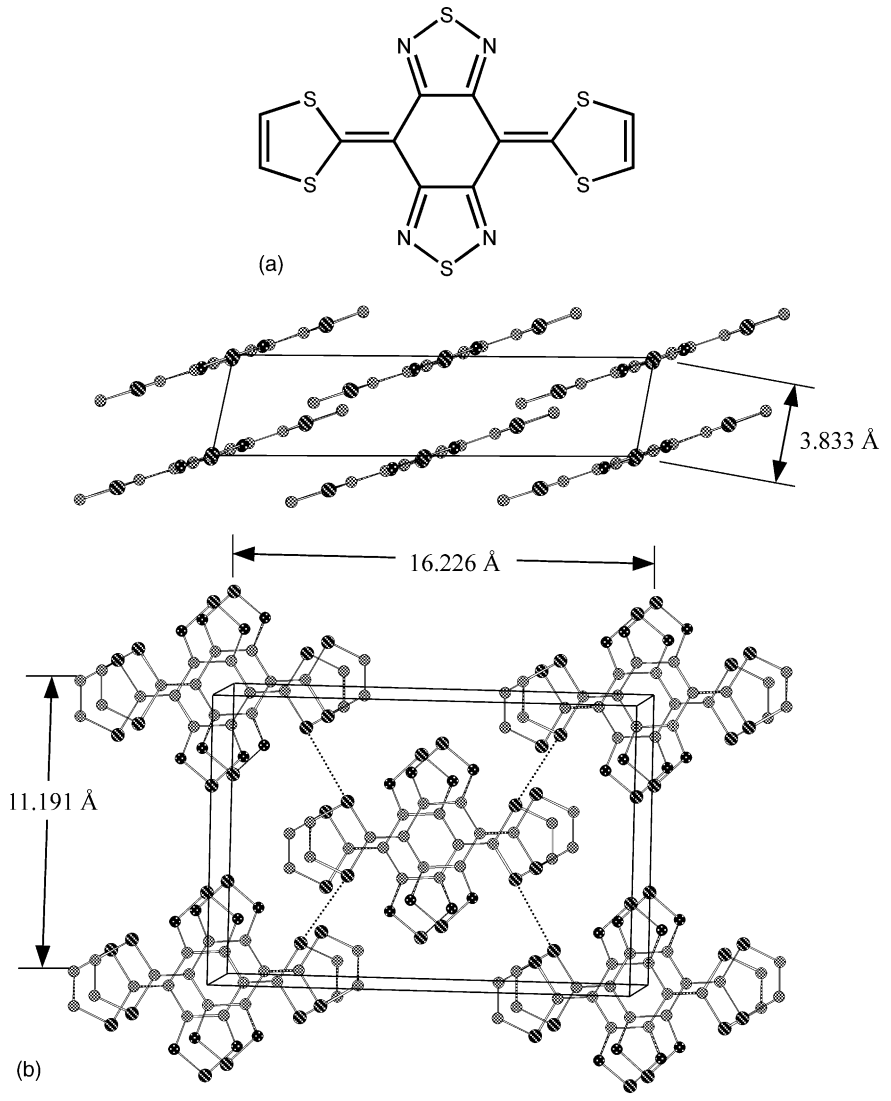

Fig. 1. (a) Molecular structure of bis(1,2,5-thiadiazolo)-*p*-quinobis(1,3-dithiole). (b) Perspective views of the BTQBT crystal structure. The BTQBT single crystal is monoclinic with lattice constants of $a = 16.226$ Å, $b = 11.191$ Å, $c = 3.833$ Å, $\beta = 96.88°$. The S···S contacts between neighboring molecules are shown as the dotted lines.

pressure ranged from 10^{-7} to 10^{-5} Pa during growth depending on the deposition rate.

A variety of substrates was used for the growth of BTQBT thin films, including highly ordered pyrolytic graphite (HOPG), glass, Si(0 0 1), and 1 μm thick silicon dioxide films grown on Si(0 0 1) wafers by wet oxidation. A 1.4 cm^2 HOPG substrate with mosaic spread (half maximum height peak width of the Cu-K_α X-ray rocking curve) less than 0.4° was cleaved in air and immediately loaded into the growth chamber via a vacuum load lock mechanism. Si(0 0 1) wafers were first immersed in a solution of sulfuric acid and 30% H_2O_2 (by a ratio of 1:1) for 10 min. Then, they were dipped in 1:50 HF:H_2O for 30 s to remove the surface oxide layer, rinsed in deionized water and blown dry, and within 30 s they were loaded into the UHV chamber. Microscope cover glass and Si

substrates with thermal oxide films were boiled in 1,1,1-trichloroethane, rinsed in acetone followed by isopropanol, and blown dry. All substrates were heated to 700 K for 20 min in vacuum to desorb surface contaminants. The substrate temperature was varied from 300 to 150 K during growth. A detailed description of the OMBD process and the deposition system can be found elsewhere [12,15].

2.2. Film characterization

In situ reflection high-energy electron diffraction was employed to study the growth evolution of BTQBT thin films grown on an HOPG substrate. The high-energy electron beam was directed onto the sample at a glancing angle of approximately 2°. The energy and the current of the electron beam were 8 KeV and 0.5 mA, respectively. At different stages of the BTQBT thin film growth, the RHEED pattern on the phosphorus screen was photographed and scanned into digital format for further image processing. The electron beam was directed away from the sample immediately after recording the RHEED pattern to prevent damage to the films, as we found that the RHEED pattern tended to fade when the exposure time of the organic layer to the electron beam exceeded several seconds.

Topographic images of surfaces of the OMBD-grown BTQBT thin films were obtained by both scanning electron (Philips XL30) and tapping-mode atomic force (Digital Instruments Nanoscope) microscopy. In the SEM measurement, 2000 Å thick BTQBT films grown by OMBD on Si(0 0 1) were coated with 100 Å thick Au layers to prevent sample charging. The root-mean-square (RMS) surface roughnesses of 500 Å thick BTQBT films grown under different conditions were also measured using AFM. Glass, Si(0 0 1), and silicon substrates coated with a 1 μm thick thermal silicon dioxide layer were used as substrates. All of these substrates had RMS surface roughnesses less than 0.2 nm, and were free of features observed using AFM.

For X-ray measurements, a Cu-K_α (at wavelength $\lambda = 1.54$ Å) X-ray source was used in a Rigaku diffractometer. The θ–2θ scans and rocking curve measurements were conducted for BTQBT films grown on glass and Si(0 0 1) substrates. To further investigate the molecular stacking order, the Schultz reflection method was used for obtaining the X-ray pole figures of the (2 0 1) and (0 2 1) crystal plane normals, the former corresponding to the stacking direction of the BTQBT molecules.

The photoluminescence spectra of a 1000 Å thick BTQBT film grown on a Si(0 0 1) substrate were measured at temperatures ranging from 15 to 280 K using an Ar^+ laser at the wavelength of $\lambda = 488$ nm as the excitation source. The PL spectra were recorded by a Hamamatsu Streak Scope C4334.

The interest in BTQBT lies primarily in its unusually high electrical conductivity and carrier mobility. Hence the electrical conductivity of the OMBD-grown BTQBT thin films was measured both perpendicular and parallel to the substrate surface at temperatures from 120 to 330 K. To measure the perpendicular conductivity, a 1500 Å thick In layer was thermally evaporated in vacuum onto a Si substrate, followed by the deposition of a BTQBT film with a thickness of between 1000 and 4000 Å by OMBD. Finally, 1000 Å thick In contacts were deposited through a shadow mask with 0.15 mm diameter circular openings. Current–voltage characteristics were measured between the bottom In layer and the top In contacts with a HP4145 semiconductor parameter analyzer. For the parallel conductivity measurement, a 1000 Å thick Au layer was thermally evaporated onto a SiO_2 surface forming parallel Au stripes spaced at 100 μm. Following the 2 Å/s deposition of a 1000 Å thick BTQBT film, current–voltage characteristics were measured between neighboring Au stripes.

3. Results

3.1. Evolution of film growth

Fig. 2(a) shows the RHEED pattern of an HOPG substrate prior to deposition, where the bright and continuous streaks are an indication of

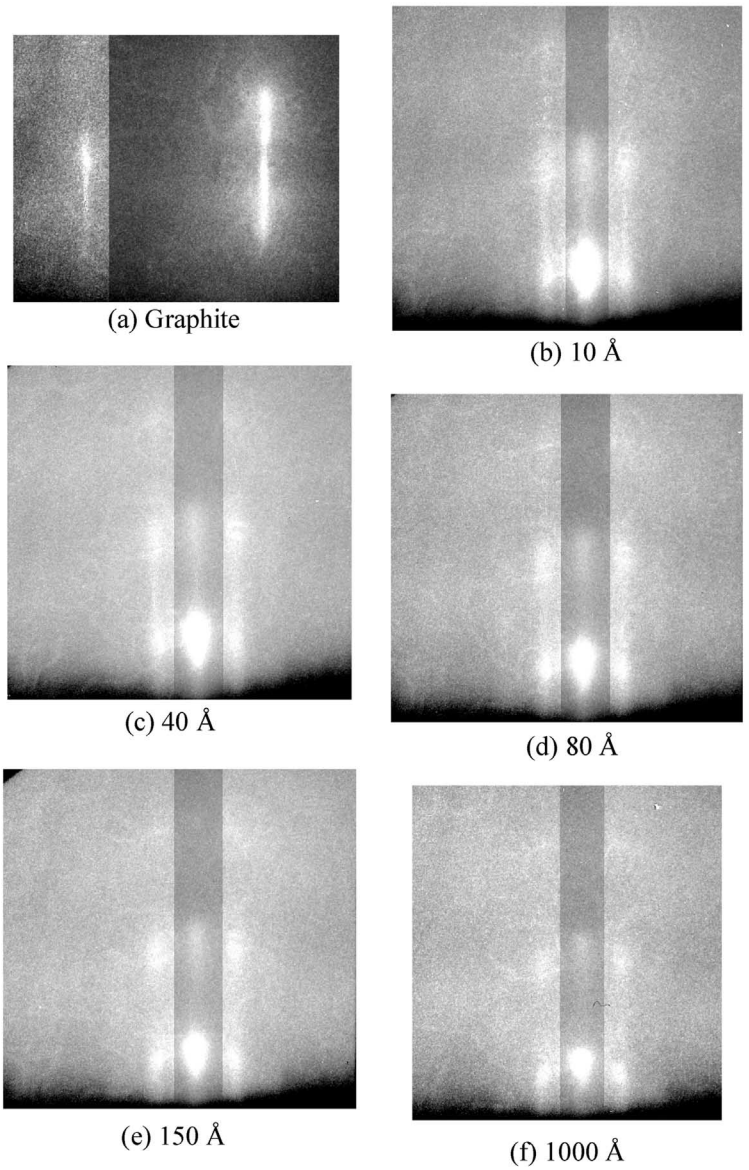

Fig. 2. The evolution of RHEED patterns during the growth of a BTQBT film on HOPG as the total thickness of the BTQBT layer increased from (a) 0 Å (bare graphite substrate) to (f) 1000 Å. The nonspecular reflections of BTQBT have been contrast-enhanced, and correspond to the (2 0) surface net of its crystalline structure.

the flatness of the graphite surface within the coherence length of the electron beam (on the order of 1 μm). The corresponding spacing between surface planes as calculated from the streak locations is 2.13 ± 0.06 Å, corresponding to the (1 1) reflection of the graphite surface net.

Fig. 2(b)–(f) shows the evolution of RHEED patterns obtained during the 3.0 Å/s room temperature growth of a BTQBT film on the HOPG surface. The graphite streaks begin to fade after ~3 Å (approximately a monolayer coverage) thick BTQBT is deposited onto the substrate. At the

same time, weak streaks corresponding to the (2 0) BTQBT surface net, appear near the (0 0) specular reflection, and intensify as the growth proceeds. The graphite features are completely replaced by a pair of narrowly spaced and long streaks due to diffraction from the BTQBT overlayer surface at a film thickness of 10 Å (about 3 ML) (Fig. 2(b)). The distance between the (2 0) planes is 9.1 ± 0.4 Å, consistent with a distance of 9.38 ± 0.01 Å in the bulk structure [4]. This is evidence that the first few layers of BTQBT are crystalline and reproduce the substrate flatness. The BTQBT RHEED features remain almost unchanged as the film thickness is increased to 80 Å (Fig. 2(c) and (d)), indicating that the organic overlayer retains a high degree of crystallinity and surface uniformity up to significant thicknesses. At thicknesses $\geqslant 150$ Å (Fig. 2(e)), however, the streaks gradually break into pronounced segments, reducing to spots at 1000 Å (Fig. 2(f)). Such discontinuous streaks indicate that the film surface is rough on the molecular scale.

We also compared the RHEED patterns of 40 Å thick BTQBT films grown on HOPG at different growth rates of 0.2 and 3.0 Å/s (Fig. 3(a) and (b)). The streaks were more continuous at the higher growth rate, which indicates a flatter surface. When the substrate temperature is reduced to 160 K, the RHEED pattern indicated considerable surface roughness (Fig. 3(c)), compared to that obtained at room temperature, a situation somewhat different from that previously observed in the growth of PTCDA [15].

3.2. Surface morphology and film crystallinity

Fig. 4 shows two SEM images of the surfaces of 2000 Å thick BTQBT films grown on Si(0 0 1) at room temperature, at growth rates of (a) 1.0 Å/s and (b) 4.2 Å/s. In Fig. 4(a), crystalline filaments form a mesh-like network, whereas the film surface is more uniform when grown at the higher rate (Fig. 4(b)). Similar differences can be seen from AFM images of two 500 Å thick films grown at room temperature and at rates of 0.7 Å/s (Fig. 5(a)) and 3.0 Å/s (Fig. 5(b)). At the lower growth rate, a high density of grains approximately 300 nm in diameter is observed, and the RMS surface roughness is 4.6 nm. At the higher growth rate, the grain size reduces to approximately 150 nm and the surface is relatively smooth with a RMS roughness of 2.3 nm. The surface of the BTQBT film grown at 150 K (Fig. 5(c)) is not as smooth as the film grown at room temperature at a similar growth rate (Fig. 5(b)).

Shown in Fig. 6 is the growth-rate dependence of the RMS surface roughness of 500 Å thick BTQBT films grown on different substrates and at different temperatures, as measured by AFM. Films grown at room temperature on Si have the

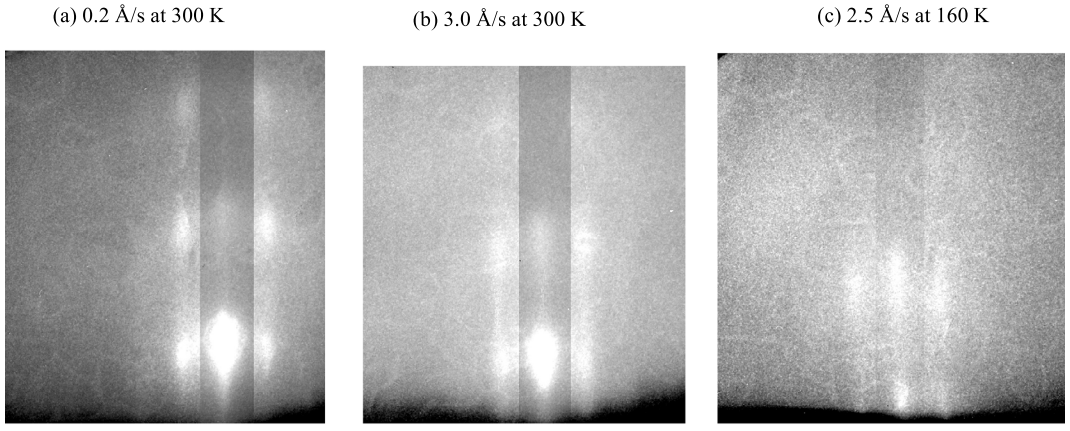

Fig. 3. RHEED patterns for 40 Å thick BTQBT films grown at different growth rates and substrate temperatures on HOPG. (a) 0.2 Å/s at 300 K, (b) 3.0 Å/s at 300 K and (c) 2.5 Å/s at 160 K.

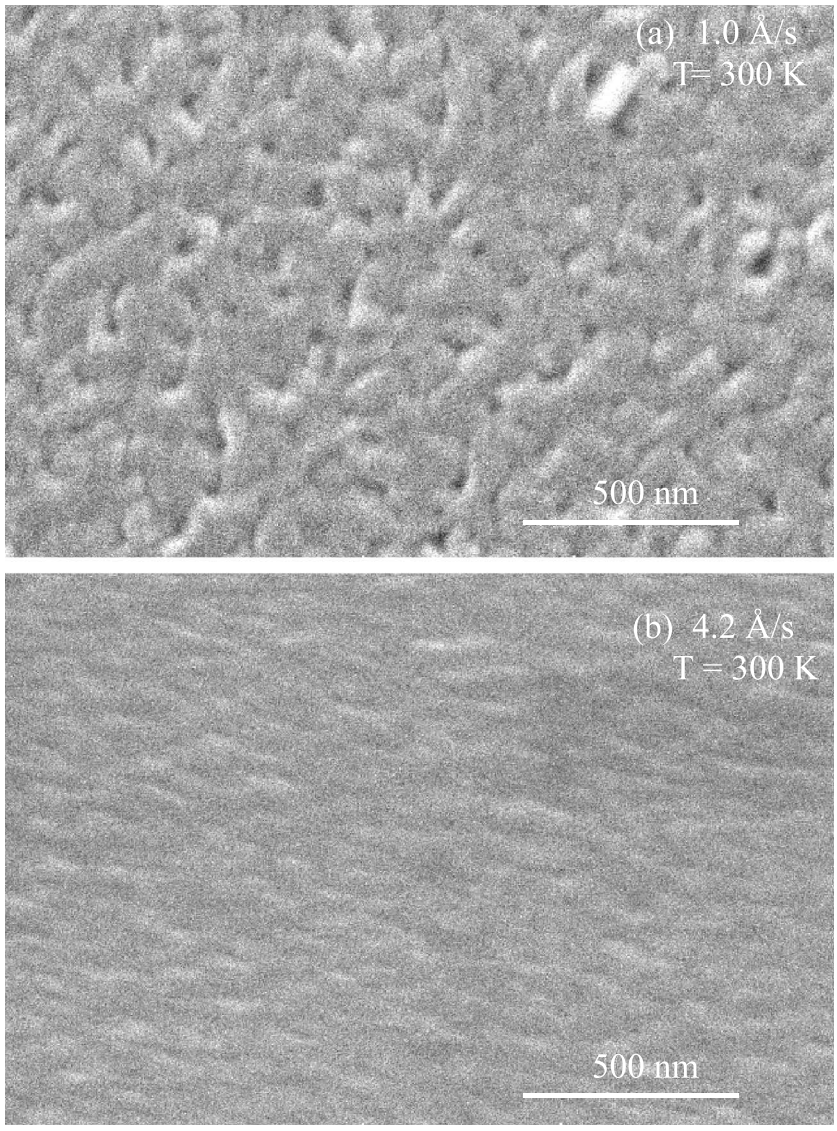

Fig. 4. SEM images of the surfaces of 2000 Å thick BTQBT films grown on Si(0 0 1) at 300 K, at a rate of (a) 1.0 Å/s and (b) 4.2 Å/s.

smallest surface roughness, while the films on glass and SiO_2 surfaces have surface roughnesses somewhat higher than the films on Si. The BTQBT film on Si grown at 150 K has a higher surface roughness than the film grown at room temperature at the same growth rate. Furthermore, the surface roughness is also observed to decrease as the growth rate increases from 0.1 to 1.2 Å/s independent of substrate, remaining approximately constant for growth rates exceeding 1.2 Å/s. This general trend shows that the growth at a high rate is favorable for achieving flat film surfaces. As a result, in all experiments to be discussed below, BTQBT films are grown at room temperature at a rate of 2 to 3 Å/s.

Fig. 7 shows two X-ray diffraction patterns of a 4000 Å thick BTQBT film grown on a glass substrate. Fig. 7(a) corresponds to the substrate

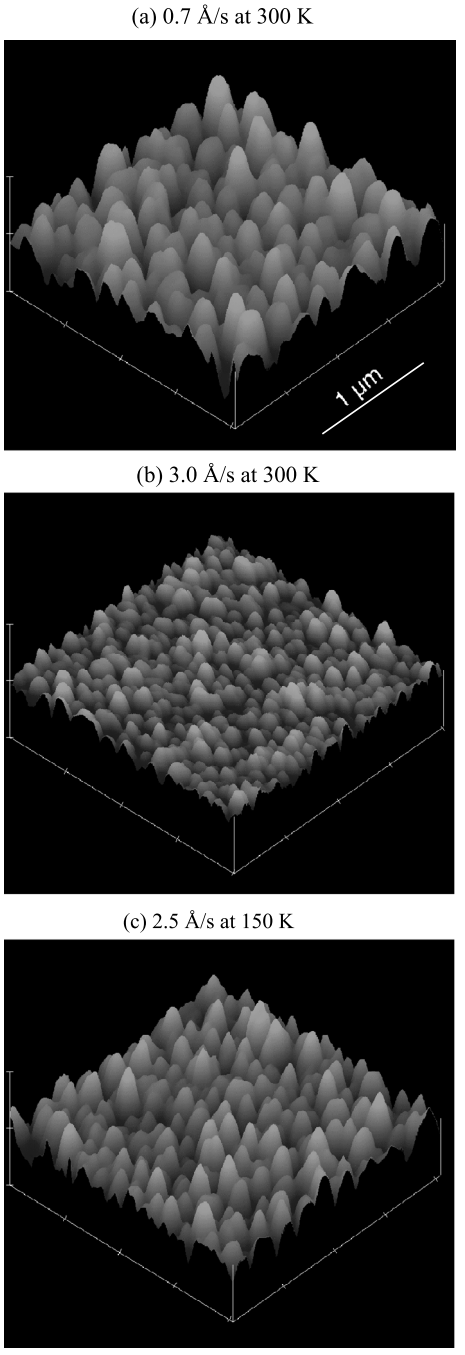

Fig. 5. Topographic AFM images of 500 Å thick BTQBT films grown on a Si(0 0 1) substrate under the growth conditions of (a) 0.7 Å/s at 300 K, (b) 3.0 Å/s at 300 K and (c) 2.5 Å/s at 150 K. The scan size is 2×2 μm^2 and the height scale is 20 nm/div in each image.

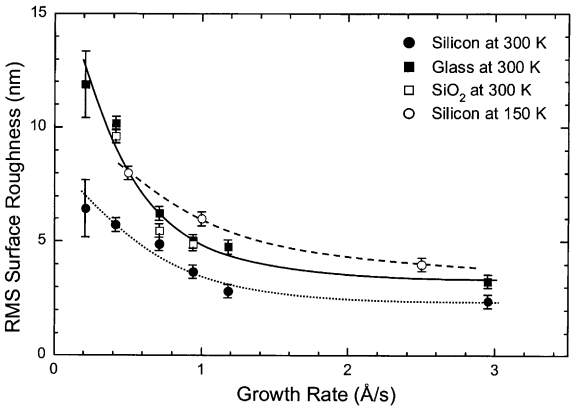

Fig. 6. The growth-rate dependence of the root-mean-square surface roughness of BTQBT films grown on different substrates at different temperatures. The symbols with error bars are the experimental data while the lines are guides for the eye.

normal lying in the plane of the X-ray beams. There is a dominant diffraction peak along with a few smaller peaks superimposed on a background signal due to diffraction from the amorphous glass substrate. The dominant peak is assigned to the (2 0 1) diffraction and is located at $2\theta = 27.04° \pm 0.05°$, corresponding to an interplanar stacking distance of $d_{201} = 3.30 \pm 0.01$ Å. This is consistent with previous measurements of the bulk stacking distance of 3.29 ± 0.01 Å [4], which indicates little or no lattice distortion in the stacking direction. The full width at half maximum (FWHM) of the (2 0 1) peak is determined to be $\delta(2\theta) = 0.30°$ by fitting its intensity profile with a Gaussian line shape. Using

$$\bar{L}_{hkl} = \frac{\lambda}{2\cos\theta\,\delta\theta},$$

where $\bar{L}_{hkl}$ is the average crystallite size perpendicular to the (*hkl*) planes and $\delta\theta$ is the X-ray diffraction peak width expressed in radians, the crystallite size perpendicular to the (2 0 1) planes is calculated to be $\geqslant 300$ Å. Since we neglected the instrumental broadening and broadening due to lattice distortions, this represents a lower limit to the crystallite size.

The existence of Bragg peaks corresponding to the (1 1 1) and (1 1 0) planes indicates some limited out-of-plane polycrystalline disorder. From the

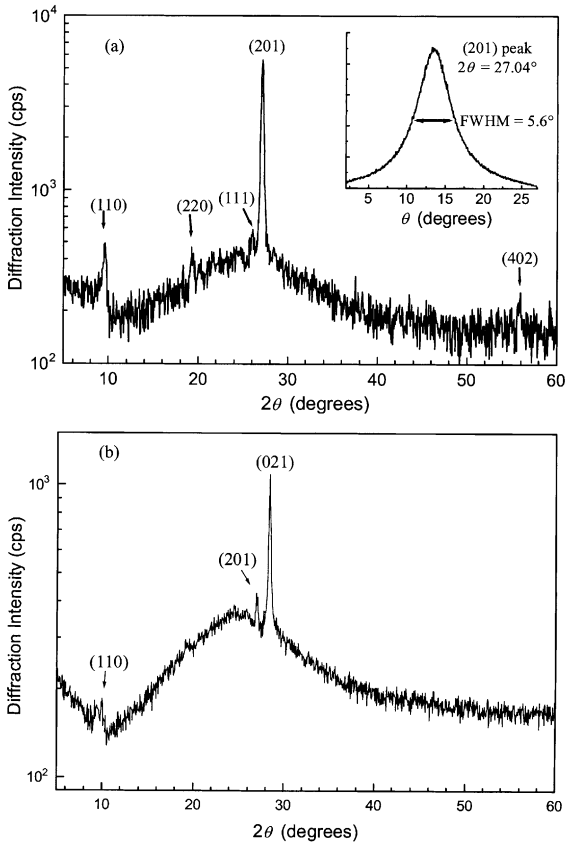

Fig. 7. X-ray diffraction patterns for a 4000 Å thick BTQBT film grown on glass at $T = 300$ K. (a) The substrate normal lies in the plane of the X-ray beams. The inset shows the rocking curve of the BTQBT (2 0 1) Bragg peak. (b) The substrate normal is tilted at 49° to the X-ray plane.

large ratio of the diffraction intensity of the (2 0 1) peak to that of the other peaks, we infer that the film orientation is characterized predominantly by the (2 0 1) plane oriented parallel to the substrate surface. Indeed, the rocking curve of the (2 0 1) Bragg peak (inset, Fig. 7(a)) shows a FWHM of 5.6°, corresponding to an angular spread in the stacking axis of only ±3°.

The significant out-of-plane order is also apparent from Fig. 7(b), where the substrate is tilted at 49° to the plane described by the incident and reflected X-ray beams. Here, the strong (2 0 1) diffraction has nearly vanished, with the diffraction pattern now completely dominated by the (0 2 1) reflection at $2\theta = 28.40° \pm 0.05°$. This corresponds to $d_{021} = 3.14 \pm 0.01$ Å, again consistent with a bulk value of 3.15 ± 0.01 Å [4].

The stacking order in BTQBT thin films is more apparent from the X-ray texture measurement. Shown in Fig. 8 are the X-ray pole figures of the (2 0 1) and (0 2 1) reflections of a BTQBT film grown on silicon. Clearly the (2 0 1) pole figure (Fig. 8(a)) suggests the molecular stacking axis is oriented at perpendicular to the substrate surface,

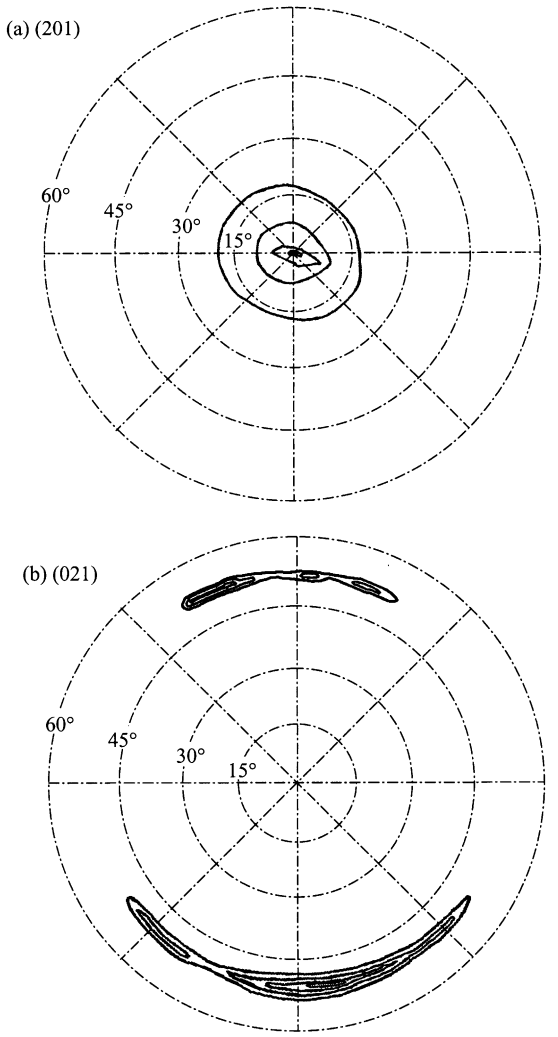

Fig. 8. X-ray pole figures of the (a) (2 0 1) and (b) (0 2 1) planes of a BTQBT thin film. In each pole figure the contours represent diffraction intensity changes of 10% of its peak intensity with the highest one corresponding to 95%. The diffraction intensity in (b) falls off quickly below 60%.

consistent with the rocking curve in Fig. 7(a). In contrast, the (0 2 1) reflection shows some distribution in intensity, although there remains a preferential azimuthal alignment with a spread of ±45°. Similar stacking order of BTQBT molecules also exists on glass substrates, although the angular distribution of the (0 2 1) reflection is slightly broader than for the films on Si. The cause of this preferential alignment is not entirely understood, although it has previously been found in the case of PTCDA to result from molecular self-organization nucleating at the edges of the substrate, or at surface patterns intentionally introduced onto the substrate [12,16].

3.3. Optical properties

A typical set of temperature dependent PL spectra of a BTQBT film grown on Si(0 0 1) is shown in Fig. 9. The $T = 280$ K fluorescence of the BTQBT film is weak and nearly featureless consisting of a broad peak centered at 1.87 eV and a shoulder at 1.50 eV. As the sample is cooled to below $T = 150$ K, the PL intensity rapidly increases, and the rather broad luminescence peak at 280 K is resolved into three narrower peaks. At $T = 15$ K, these three peaks center at 1.69, 1.83 and 1.96 eV, corresponding to a spacing of 0.14 ± 0.01 eV. This is consistent with the intramolecular C–C stretch mode typical of many planar molecules consisting of conjugated electron systems [17]. The strong temperature dependence of the PL spectra is attributed to the reduced exciton–phonon interactions with decreasing temperature. In planar molecules such as PTCDA [18] and BTQBT, strong coupling exists between excitons and intramolecular phonon modes. Phonon-enhanced internal conversion provides a nonradiative transition path for excitons, leading to luminescence quenching at high temperatures.

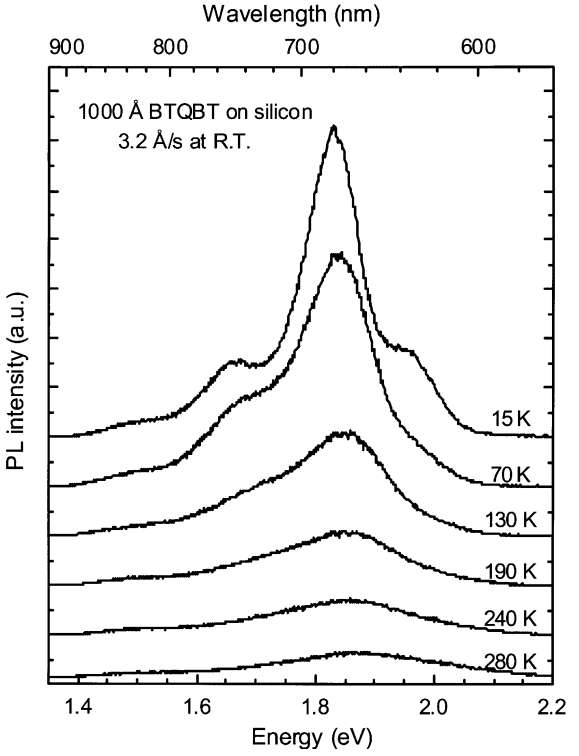

Fig. 9. A typical set of temperature-dependent photoluminescence spectra of a 1000 Å thick BTQBT film grown on Si(0 0 1) at 3.2 Å/s at 300 K.

3.4. Electrical properties

The current–voltage (I–V) characteristics in both the perpendicular and parallel conductivity measurements are linear between ±50 V and up to a current of ±20 mA. This implies that the conduction through the film is ohmic, and that the contact resistance (which would lead to a deviation from linearity) does not dominate the electrical properties in either the vertical or in-plane contact geometries. The electrical conductivity of the OMBD-grown BTQBT film can thus be deduced from the slope of the I–V curve given the film thickness and the contact geometry. At 300 K, the vertical and in-plane conductivities of the as-grown films are $(1.2 \pm 0.1) \times 10^{-3}$ and $(7.5 \pm 0.4) \times 10^{-4}$ S cm^{-1}, respectively. The temperature dependence of the conductivity of the BTQBT film in the temperature range of from 120 to 330 K is shown in Fig. 10. Both the vertical and in-plane conductivities are thermally activated, with an activation energy of $E_a = 0.19 \pm 0.1$ eV for the vertical conductivity and $E_a = 0.18 \pm 0.1$ eV for the in-plane conductivity, both of which are very close to that previously reported for a single crystal, where $E_a = 0.21$ eV [7].

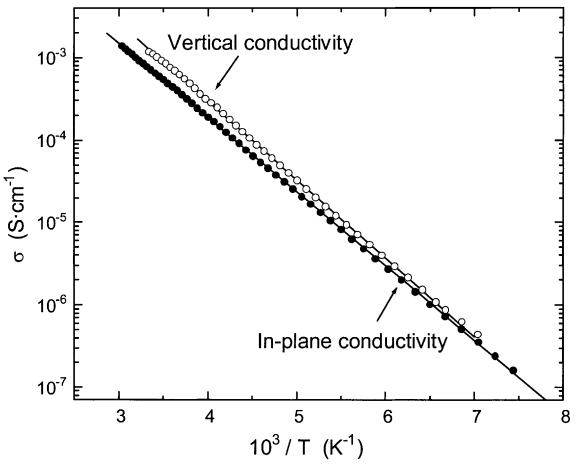

Fig. 10. The temperature dependence of the vertical and in-plane conductivities of BTQBT films grown at 2 Å/s at 300 K by OMBD. The dots are experimental data while the solid lines are linear fits of $\ln\sigma$ versus T^{-1}.

4. Discussion

4.1. Ordered growth of BTQBT films

Our experiments show that ordered BTQBT thin films can be achieved on a variety of substrates by OMBD, even though the organic overlayer and substrate are lattice mismatched. This provides evidence beyond that observed for other planar stacking organic materials that ordered growth is a general property of a large range of planar molecules that are bonded primarily by van der Waals forces to the substrate [12].

The degree and extent of layer ordering of organic films has been shown to be strongly dependent on substrate preparation and growth conditions [13,15]. From RHEED, SEM and AFM measurements, we find that like several other organic systems, high growth rates are advantageous for obtaining uniform and ordered BTQBT films. Unlike previous experiments with PTCDA, however, we find that the growth at low temperature does not help to improve the surface flatness and ordering of the films. This behavior might be related to the strong intermolecular interaction in the lateral direction of the planar BTQBT molecules. The so-called "quasiepitaxial" growth mode is a kinetically controlled process in which the resulting structure of thin films depends on a balance between the bond and the thermal energies [12,19]. Due to the strong intralayer interaction resulting from S···S contacts, the diffusion of molecules is inhibited at a low temperature. In that case, the growth mode is likely to be layer-plus-island (Stranski–Krastanov), as opposed to layer-by-layer, and the film is less likely to be uniform than, for example, when grown at room temperature. The primary question remains as to why limited azimuthal order is observed even on amorphous substrates such as glass. One possibility is that the strong intermolecular bonds lead to lateral and rapid self-assembly of crystallites once nucleation at a substrate defect has occurred. The alignment of the crystallites on the substrate may be a result of nucleation along edges, or along surface patterns unintentionally introduced during substrate cleaning, etc. This crystal alignment is a phenomenon observed previously in the growth of films of PTCDA [12,16], NTCDA [20], DAST [21], etc., and may have origins similar to that responsible for the alignment of liquid crystal molecules deposited on brushed polymer substrates [22].

4.2. Comparisons of the electrical properties of bulk and thin film BTQBT

The electrical conductivity of a BTQBT crystal grown by recrystallization in nitrobenzene solution was reported to be $8.3 \times 10^{-4}\ \mathrm{S\,cm^{-1}}$, with a small anisotropy $\sigma_\perp:\sigma_\parallel \approx 2$ where $\sigma_\perp$ and $\sigma_\parallel$ are the conductivities along the interlayer (or along the molecular stacking axis) and intralyer directions, respectively [7]. Our conductivity measurements show that the OMBD-grown BTQBT thin films retain the high conductivity of the single crystal, with a conductivity anisotropy of $\sigma_\perp:\sigma_\parallel \approx 1.6$. This similarity between the film and bulk is a result of the high degree of stacking order in the thin films. The somewhat higher conductivities of the films (by approximately a factor of 1.4) may be due to improved purity or reduced contact resistance to the thin film samples. In either case, such a low anisotropy is once again a consequence of the strong intermolecular interaction due to the S···S contacts between adjacent BTQBT molecules.

The measured activation energy of $E_a = 0.2$ eV implies that the dominant contribution to the electrical conduction of both the BTQBT thin film and the single crystal is extrinsic, since this value is considerably less than the HOMO–LUMO energy gap of $E_g = 2.1$ eV, as estimated by the low energy optical absorption edge of the material. As Hall measurements of single crystal samples indicate that the dominant carriers in BTQBT are holes [7,8], this suggests that the conductivity arises from thermal excitation of holes from deep levels located at approximately 0.2 eV above the HOMO. The origin of this deep level is not clear.

5. Conclusion

We have described a detailed characterization of the various structural, optical and electrical properties of BTQBT thin films grown by organic molecular beam deposition. We have shown that BTQBT thin films can be grown into ordered structures independent of lattice matching with the underlying substrate. The planar BTQBT molecules form ordered stacks whose axis lies perpendicular to the substrate surface. The degree and extent of film ordering strongly depend on the growth conditions. Higher growth rates favor more ordered and uniform films. We have also shown that the OMBD-grown BTQBT thin films retain the high conductivity and low anisotropy of the single crystal, both of which are consequences of the strong intermolecular interaction arising from the S···S contacts between neighboring molecules.

Acknowledgements

The authors thank Peter Peumans for assistance with the thin film growth, and Prof. Chihaya Adachi for help with the optical measurements. We also thank the Air Force Office of Scientific Research and the National Science Foundation MRSEC program for partial support of this research.

References

[1] E.A. Silinsh, V. Capek, Organic Molecular Crystals: Interaction, Localization and Transport Phenomena, Springer, Berlin, 1995.
[2] J.H. Schön, C. Kloc, B. Batlogg, Science 288 (2000) 2338.
[3] F.F. So, S.R. Forrest, Mol. Cryst. Liq. Cryst. Sci. Technol. B 2 (1992) 205.
[4] Y. Yamashita, S. Tanaka, K. Imaeda, H. Inokuchi, Chem. Lett. (1991) 1213.
[5] H. Inokuchi, Mol. Cryst. Liq. Cryst. 255 (1994) 187.
[6] H. Inokuchi, K. Imaeda, Acta Phys. Pol. A 88 (1995) 1161.
[7] K. Imaeda, Y. Yamashita, Y. Li, T. Mori, H. Inokuchi, M. Sano, J. Mater. Chem. 2 (1992) 115.
[8] K. Imaeda, Y. Li, Y. Yamashita, H. Inokuchi, M. Sano, J. Mater. Chem. 5 (1995) 861.
[9] H. Fujimoto, K. Kamiya, S. Tanaka, T. Mori, Y. Yamashita, H. Inokuchi, K. Seki, Chem. Phys. 165 (1992) 135.
[10] S. Hasegawa, T. Mori, K. Imaeda, S. Tanaka, Y. Yamashita, H. Inokuchi, H. Fujimoto, K. Seki, N. Ueno, J. Chem. Phys. 100 (1994) 6969.
[11] N. Ueno, Jpn. J. Appl. Phys. 38 (Suppl. 1) (1999) 226.
[12] S.R. Forrest, Chem. Rev. 97 (1997) 1793.
[13] S.R. Forrest, Y. Zhang, Phys. Rev. B 49 (1994) 11297.
[14] Y. Yamashita, S. Tanaka, K. Imaeda, H. Inokuchi, M. Sano, J. Org. Chem. 57 (1992) 5517.
[15] S.R. Forrest, P.E. Burrows, E.I. Haskal, F.F. So, Phys. Rev. B 49 (1994) 11309.
[16] R.B. Taylor, Z. Shen, S.R. Forrest, IEEE Photonics Technol. Lett. 9 (1997) 365.
[17] K. Akers, R. Aroca, A.-M. Hor, R.O. Loutfy, J. Phys. Chem. 91 (1987) 2954.
[18] V. Bulovic, P.E. Burrows, S.R. Forrest, J.A. Cronin, M.E. Thompson, Chem. Phys. 210 (1996) 1.
[19] P. Fenter, F. Schreiber, L. Zhou, P. Eisenberger, S.R. Forrest, Phys. Rev. B 56 (1997) 3046.
[20] R. Strohmaier, C. Ludwig, J. Petersen, B. Gompf, W. Eisenmenger, Surf. Sci. 351 (1996) 292.
[21] S.R. Forrest, P.E. Burrows, A. Stroustrup, D. Strickland, V.S. Ban, Appl. Phys. Lett. 68 (1996) 1326.
[22] M.B. Feller, W. Chen, Y.R. Shen, Phys. Rev. A 43 (1991) 6778.